

THE STONE ROOF OF THE *THOLOS* OF ATHENA PRONAIA IN DELPHI: STRUCTURAL HYPOTHESES STARTING FROM FRAGMENTS OF MARBLE TILES

D. Aita ^{1*}, V. Beatini ², E. Garavaglia ¹, V. Paris ³, A. Pizzigoni ⁴, L. Sgambi ⁵

¹ Politecnico di Milano, Department of Civil and Environmental Engineering (DICA), 20133 Milano, Italy
(danila.aita, elsa.garavaglia)@polimi.it

² Aarhus University, Department of Civil and Architectural Engineering, 8000 Aarhus C., Denmark - valentina.beatini@cae.au.dk

³ University of Bergamo, Dipartimento di Ingegneria e Scienze Applicate, 24044 Dalmine (BG), Italy - vittorio.paris@unibg.it

⁴ University of Bergamo, Italy (former professor) - attilio.pizzigoni@gmail.com

⁵ Université catholique de Louvain-la-Neuve, Louvain research Institut for Landscape, Architecture, Built Environment,
7500 Tournai, Belgium - luca.sgambi@uclouvain.be

KEY WORDS: *Tholos* of Delphi, Roof stone tiles, Wood, Conical dome, Elastic analysis, Limit analysis, Interlocking masonry, Structural archaeology.

ABSTRACT:

This contribution is the first step of a multi-disciplinary research project, aimed at studying the roof of the *tholos* of Athena Pronaia in Delphi, dating back to the first decades of the 4th century BC. The starting point of this research is the fascination exerted by the tectonic quality of the temple, comprising some complex fragments of marble tiles belonging to the roof of the *tholos*. Despite the number of studies on this sanctuary, the poor state of preservation and lack of original material did not allow archaeologists to perform concluding research on its original configuration, in particular with reference to the reconstruction of the roof. Aware of the complexity of this topic, this contribution aims at exploring two possibilities, namely, on the one hand, that the fragments of tiles constitute elements supported by a wooden structure, and on the other hand, that they are structural elements of a stone system subjected to compressive stresses. Our contribution intends to serve as food for thought on the need for archaeological studies to be accompanied not only by advanced surveys in the field, aimed at the precise definition of the geometry of the finds, but also by architectural and structural investigations which make it possible to verify the feasibility of the hypothetical reconstructions of the architectural elements aware of the construction techniques used in the past.

1. INTRODUCTION

The study of ancient architectural structures is an area of broad impact. Whereas sociologists shed light on the ancient sociocultural *milieu*, engineers, and architects get information on local, often dismissed construction methods, which may further inspire novel sustainable technologies. In the cases of limited, broken, and sometimes even apparently contradicting findings, developing a hypothesis on the composition of the original structure can pose overwhelming difficulties. This is the case with the *tholos* of Athena Pronaia in Delphi, the object of this research. Constructed around the IV BCE, the *tholos* became an archetype of rounded structural typologies and originated various examples spanning from ancient Greece to nowadays.

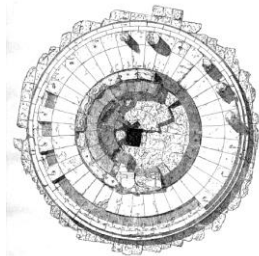


Figure 1. Plan view of the *tholos* from the survey by Charbonneaux and Gottlob (1925).

The temple, unfortunately, collapsed in ancient times. The plan from the first survey, pursued by the *École Française d'Athènes* in 1925 (Charbonneaux and Gottlob, 1925) is illustrated in Figure 1. In 1938, three fallen columns and part of the architrave were relocated over the stylobate during the archaeological campaign run by same institution.

Other findings, many of which are fragments of carved stones, lie on site and in the nearby Delphi Archaeological Museum.

Given the prominence of the temple, it may have been possible that novel or complex solutions characterized its structure. Archeologists (Gottlob, Roux, 1952; Kirk, 1968; Hoepfner, 2000; Bommelaer, 2015; Tarryn, 2018) have been developing and confronting hypotheses on the possible original image of the temple, and yet a conclusive result has not been reached. The reasons are multiple. There are intrinsic limits to surveying techniques at the times the hypotheses have been developed. In this regard, Tokmakidis et al. (1998) describe one of the first surveys applying photogrammetry, which was performed on the *tholos*. Ito et al. (2004) stressed the need for integrated research and chose again some of the findings of the *tholos* to test what new results digital photogrammetry tools could achieve. Today, a full digitalized survey has not been completed.

The major uncertainties regard the structure of the roof. Scholars have debated over the role of interlocking tiles (Figure 2) as well as the presence of two different *sima*. The number of columns and the height of the wall of the cell have also been questioned. Moreover, the possible reconstructions have not been subjected to structural analyses, which has made it difficult to prove the feasibility of the hypotheses. In the following Section, the starting point is the visualization of the factor of tectonic quality of the structure, and the reporting of the uncertainties from the survey campaigns that affect the development of hypotheses. Eventually, to introduce the potentialities of an interdisciplinary approach, this paper discusses two substantially different structural solutions that could fit one of the most accredited reconstruction hypotheses: in Section 3, the possibility of a wooden structure, in Section 4, the one of a stone structure.

Results are summarized in the concluding remarks, together with reflections on the validity of the approach.

2. HYPOTHESES ON THE STONE ROOF

2.1 The tectonic qualities of the *tholos*

A brief description of the key characteristics of the *tholos* allows an understanding of its architectural level. The temple is a perfect example of tectonic design (Kristensen and Kirkegaard, 2013): it links architectural qualities to structural expression via form, material, and details. The materials were chosen with high care: the elevation was built from white Pentelic marble on a dark Eleusis stone stylobate, allowing for strong colour contrasts. The decoration of the structure is also excellent. Such quality may match its algebraic complexity. As typical in ancient Greece, geometrical modules rule the relationships among the parts. Vitruvius in his book VII reports that the architect, Theodoros of Phokaia, authored a treatise titled *De Symmetriis*. Bosquet (1993) carried out a careful study on the survey and demonstrated how the drawing process of two concentric pentagons fits the positioning and sizing of all elements of the stylobate, from the diameter of the cell up to the arrangement of its stones. The likeliness of the construction process is validated in (Osthues, 2014). Euclid drew the icosahedron starting from two interlacing pentagons; Pizzigoni et al. (2022a) and Pizzigoni (2023) proposed to extend the role of proportions to the third dimension employing an icosahedron.

2.2 Major variations in the interpretations

Hypotheses concerning the shape of the roof started with the first, analogical survey by Gottlob. Focusing on the two *sima*, and assuming them located in two different positions, Gottlob proposed a double roof, one part spanning over the peristyle to the wall of the cell, and one covering the cell. The finding of the statue is placed to conclude the smaller roof. Eventually, other roof images followed, in a series of reminders and revisions. A few ones turn around the concept of a conical or frustoconical roof. They have first been proposed by Roux and Kirk respectively, as a result of a survey conducted by the *École Française d'Athènes* in 1952. Kirk further delved into the modelling of the tiles, which he first interpreted as flat tiles. A diverse image is that suggested by Laroche (Bommelaer, 2015). The most technically detailed archaeological reconstruction is perhaps the one by Hoepfner (Hoepfner, 2000). The image that he proposes is that of a double, conical roof, and it is taken as a reference for these structural studies.

2.3 The double roof

The reconstruction hypothesis developed by Hoepfner is reported in Figure 3: there is a very low double roof, one central part covering the cell, and one outer part one part overhanging from the peristyle. There is no height discontinuity between the two roofs. The two *sima* find their function each as a gutter of one of the two roofs.

The hypothesis of the archaeologist finds its reasoning in the constructability of a circular roof via stone roofing, Figure 4. The complex joints of the tiles shall match. Therefore, assuming the tiles to be arranged into circular rows, they shall be smaller and smaller in size to fit the decreasing dimensions of the roof. Consequently, the stone dimensioning and carving processes can become quite complex. The difficulties can be limited by dividing the roof into two parts and starting over with larger tiles at the outer border of the roof of the cell.

Hoepfner suggests that the roof was carried by a radial framework of wooden beams. As he pointed out, joining the beams at the top of the roof would also be difficult, and even more importantly, it could result in an unstable structure. He suggests that the double roof may again have been chosen to solve the problem: ring support at the intersection of the two roofs allows for interrupting one beam every two, consequently facilitating the joining at the top.

Recently, a contribution from the architectural engineering community suggested that tiles of that kind may act as structural elements per se, arranged into a circular stone dome (Pizzigoni, Beatini, and Paris, 2022a; Pizzigoni, Paris and Beatini, 2022b; Pizzigoni, 2023).

To consider the most diverse structural hypotheses, the proposed roof will be discussed in Section 3 as made of stone tiling and wooden substructure, and in Section 4 as composed of structural stones.



Figure 2. The largest of the stone tile findings.

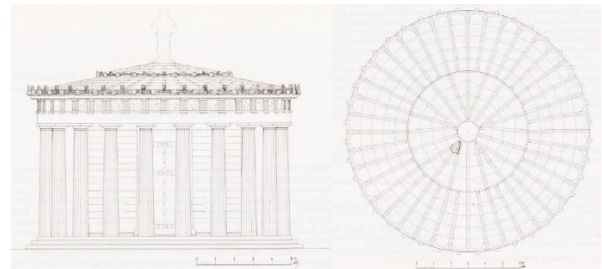


Figure 3. A proposal of roof reconstruction according to Hoepfner (2000).

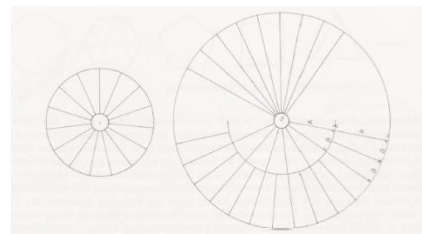


Figure 4. Increasingly smaller tiles towards the centre of the roof. From (Hoepfner, 2000).

3. THE ROOF AS A WOODEN STRUCTURE

3.1 Assessment method

The first hypothesis investigated is the wooden structure proposed by Hoepfner, Figure 3. In this contribution, a preliminary structural analysis is performed by adopting a linear elastic model. The sectional analysis, useful for a pre-dimensioning, or a rough verification of the load-bearing capacities, is performed using the permissible stress approach; the design values for the permissible stresses are reduced by a suitable safety factor, see Tables 1, 2, and 3 below. It did not seem appropriate to carry out a limit state analysis as it would result in too severe requirements for the 'good building' rules in force at the time of the construction. The analysis investigated the

equilibrium conditions, the compatibility conditions, the bearing capacity of each structural element, and subsequently the possible loss of stability due to unopposed horizontal thrusts. The roof is modelled using planar structural schemes: each beam is analyzed for its ability to carry the loads in its tributary area.

The schemes are reported in Figure 5: the area related to one slope of the central roof is in blue; the area related to one beam of the external roof is in yellow.

Given the weight of the stone tiles, the contribution of variable loads is disregarded and just dead loads are considered. These are determined by taking into account the stone roof, assuming a thickness of 21 cm and a specific weight of 26 KN/m³, and the wooden elements (loads that are however negligible compared to the load of the stone). Concentrated vertical loads are assumed at the outer end of the beam to read for the weight of the highly decorated *sima*, the *geison*, and possible *acroteria*.

Over the twenty columns, it shall be assumed the presence of horizontally laid structural elements (toric lintel) supporting the forty overhanging beams. The assumed average elastic moduli are: $E_{wood} = 10000$ MPa; $E_{stone} = 2850$ MPa.

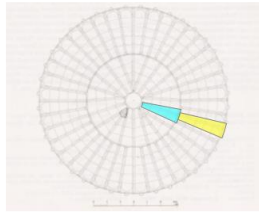


Figure 5. Tholos roof and areas of influence of the loaded beams (re-elaboration from Hoepfner, 2000).

3.2 Linear static analysis

3.2.1. Structural scheme: The structural scheme of the roof is illustrated in Figure 6a. A lowered double-pitched beam carries the central part of the roof; it is subjected to the vertically distributed loads and rests over the cell. The external part is schematized as a beam resting on the wall and the perimeter column, subjected to vertically distributed loads and a point load at its outer end. The beam is overhanging, as by Hoepfner (2000) (Fig. 3). Two causes of failure may arise. Firstly, the load on the beams may be excessive. Secondly, as illustrated in Figure 6b, the deformations produced by the loads in the central lowered double-pitched beam may turn into an overturning horizontal force acting on the vertical support elements, initiating a collapse mechanism.

3.2.2. Roof elements: Figure 7 illustrates in detail the structural schemes of the single elements. To ensure equilibrium, the outer beam has a hinge support at the top and a roller support at the bottom, which read for the support provided by the internal wall and external column respectively. The beam is set to have a solid cross-section of 20 cm x 25 cm. The central beam is schematized as simply supported. This allows for assessing the occurrence of horizontal sliding on the wall as well as the suitability of the wall to resist the thrust. For equilibrium, a roller support was added at the top. In this case, the wooden element is thought to have a section size of 25 cm x 30 cm. The analyses demonstrate that the beams are in equilibrium, Figure 8. The sectional bending, axial and shear stresses are well within the admissible limits (Tab. 1). The sections were also verified under combined bending and axial loading (both tensile and compressive) without any material strength issues being found (Tab. 2).

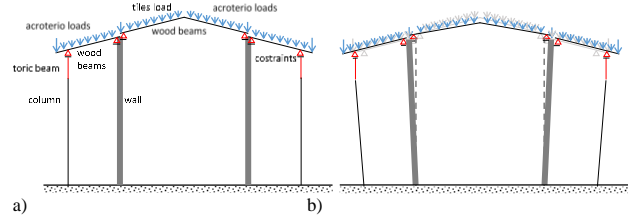


Figure 6. (a) Possible static configuration and (b) plausible collapse mechanisms.

Table 1. Sectional analysis: bending (f_m), tension parallel to the fibers (f_{t0}), compression parallel to the fibers (f_{c0}), and shear (f_v).

Strength (N/mm ²)	f_m	f_{t0}	f_{c0}	f_v
Design limit values*	9.60	5.60	8.40	3.70
External beam	3.07	0.052	0.040	0.32
Central beam	5.63	0.0	0.045	0.42

* Reference: Table D24- UNI EN 338-2016

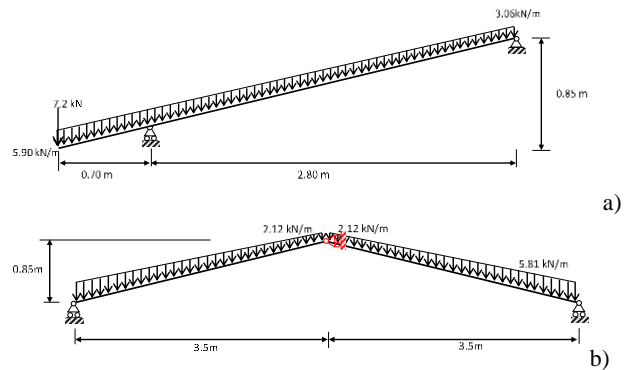


Figure 7. Static schemes: a) external beam; b) central beam.

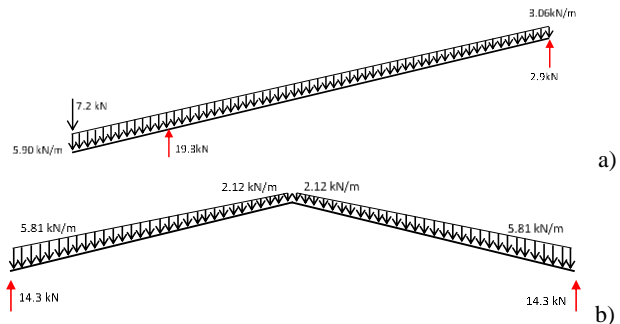


Figure 8. Static equilibrium of roof structures: a) external beam; b) central beam.

Table 2. Sectional analysis: combined bending and axial loading.

Strength (N/mm ²)	Maximum tensile stresses	Maximum compressive stresses
Design limit values*	9.60	9.60
External beam	3.12	0.66
Central beam	5.67	0.0

* Reference: Table D24- UNI EN 338-2016

Table 3. Sectional analysis: vertical structures

Resistance (N/mm ²)	f_c	f_v	f_{critic} column	f_{critic} wall
Design limit values*	7.0	0.023	7.35	4.9
Column	0.3	0	0.3	
Wall	0.24	0		0.24

* Reference: Table D24- UNI EN 338-2016

The second analyses concern the elastic deflections of the structure. This is compared with the control values typical of modern engineering standards, i.e., for the simply supported beam, deflections: $D_{ya-a} = 1/250$ of the span; for the overhanging beam: $D_{ys} = 1/500$ of the span; for the external beam the above relations provide: $D_{ya-a} = 2890 / 250 = 11.6$ mm; $D_{ys} = 720 / 500 = 1.44$ mm; finally for the central beam: $D_y = 3600 / 250 = 14.4$ mm. The values recorded by the deformation analysis, reported in Figure 9, are lower than the control ones except for the deflection at the crown. This reaches a vertical displacement greater than the admissible one; however, it should be considered that the magnitude of this displacement is a few centimetres and refers to a standard that is certainly more restrictive than the rules applied at the time of construction.

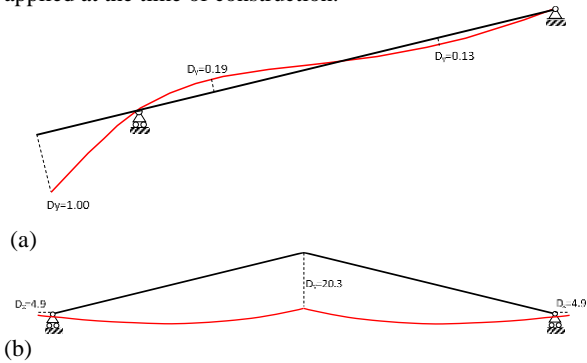


Figure 9. Vertical and horizontal displacements: (a) external beam; (b) central beam.

3.2.3. Vertical supports: Once ensured the beams are structurally acceptable, it shall be verified that the vertical supports, i.e., the column, and the cell, can carry them. Both are in stone and rest on the ground. In the analysis, the following dimensions are assumed: a diameter of 75 cm for the column and a thickness of 75 cm for the wall. Their structural scheme is illustrated in Figure 10.

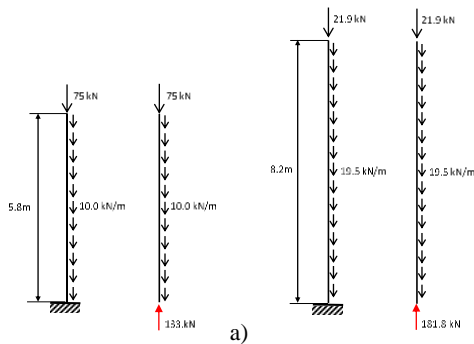


Figure 10. Static schemes of vertical supports: a) external column; b) internal wall.

The loads to which the two elements are subjected are: for the perimeter column, the load transmitted by the roof through the constraints, the weight of the edge lintel and the column's self-

weight; for the internal wall, the analysis refers to a portion of one meter of the wall which is subjected to the loads transmitted by the central beam, the external beam, the innermost *geison*, and the weight of the portion of the wall considered.

The sectional analysis does not highlight any problems: both the stress state and the deformation state are far below the assumed design limits. As regards the vertical deformations, they are contained for both elements within 0.02 mm. Even the buckling analysis does not reveal any critical issues (Tab. 3).

3.3 Investigation on the activation of possible collapse mechanisms

The second analysis regards the horizontal displacement recorded in the central beam, Fig. 9b. This, even if of a limited entity, should be contrasted with horizontal reactions opposite to the sliding direction. These forces can be generated by the constraint itself by assuming a stone-wood interface, whose friction coefficient is set as $\mu = 0.7$. The analysis starts from the external column, modelled as a homogeneous element along its entire height. Assuming that the rotation occurs at the base of the column according to Figure 11a, to respect the rotational equilibrium condition it is necessary that the shear force, X , at the top, satisfies the inequality:

$$Q \cdot \frac{d}{2} \geq X \cdot H \quad (1)$$

where Q is the sum of the vertical, stabilizing actions on the column, and d and H are the diameter and height of the column, respectively. Thus,

$$X \leq \frac{Qd}{2H} \quad (2)$$

The maximum shear force that the column can bear without overturning is $X = 8.59$ kN.

The beam could transmit a horizontal force $R_1 = \mu \cdot R_2$, where $R_2 = 19.3$ kN is the vertical reaction of the beam in Figure 8a. Therefore, the friction force that could occur is $R_1 = 13.51$ kN. From the above, the probability of overturning could exist.

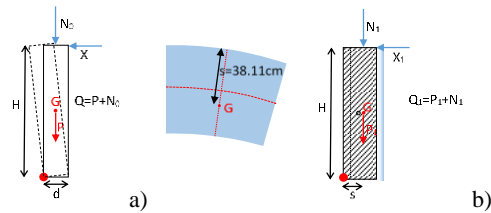


Figure 11. Schemes of the overturning mechanism: a) column; b) portion of the wall.

To assess whether the thrust exerted by the internal portion of the roof can activate this kind of mechanism, the verification against overturning is performed also on a portion of the central wall. The analysis, conducted by considering only a portion of the wall, is certainly in favour of safety as the circularity of the wall should guarantee greater inertia to overturning.

By adopting the same procedure used for the column, it can be demonstrated that the collapse mechanism of the wall (Fig. 11b) could be induced by a horizontal force, X_1 , equal to:

$$X_1 \leq \frac{Q_1 s}{H} = \frac{181.8 \cdot 38.11}{820} = 8.45 \text{ kN.} \quad (3)$$

Again, the beam-to-wall constraint is assumed to be a frictional contact with a friction coefficient $\mu = 0.7$. In this case, the beam

could transmit a horizontal force, R_3 , on the internal wall equal to

$$R_3 = \mu \cdot R_4 = 0.7 \cdot 14.3 \text{ kN} = 10.01 \text{ kN}, \quad (4)$$

where R_4 is the vertical reaction in Figure 8b. Also in this case the portion of the wall investigated could be subjected to overturning. However, the reactive horizontal force that the external beam could provide to prevent overturning has to be taken into consideration. Always assuming that the constraint is a frictional contact and that the wall transmits the horizontal thrust of the internal beam to the external beam, the frictional constraint of the external beam would produce on the wall a reaction, R_5 , opposite to the thrust, equal to (Fig. 12):

$$R_5 = 0.7 \cdot R_6 = 0.7 \cdot 2.9 = 2.03 \text{ kN}. \quad (5)$$

The sum of the two horizontal forces gives a force on the wall equal to $R = R_5 - R_3 = -7.98 \text{ kN}$ in the opposite direction with respect to the thrust of the internal portion of the roof. Since the overturning limit force of the wall, $X_1 = 8.45 \text{ kN}$, is less than the value of R thus obtained, the stability of the wall is guaranteed as well as the horizontal reaction contrasting the thrust (Fig. 12).

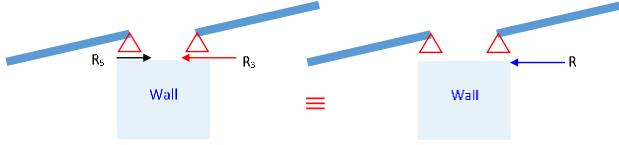


Figure 12. Diagram of the transmission of horizontal forces on the central wall by friction.

The thrust of the wall on the external beam is also transmitted to the beam-column constraint with the same intensity. For the column, the overturning limit is represented by a force equal to 8.59 kN. The transmitted force being equal to the friction reaction, $R_5 = 2.03 \text{ kN}$, under the action of the investigated loads, the stability of the column is guaranteed.

Once again it is underlined that the stability of the wall is studied on an isolated portion of the wall. The almost complete circularity of the wall is certainly an aspect in favour of safety.

4. THE ROOF AS A STONE STRUCTURE

This Section aims to verify whether the double roof could have been composed of self-supporting marble tiles as compressed structural elements.

4.1. Durand-Clayé's stability area method

The method employed to assess the equilibrium of the *tholos* roof, conceived as a stone structure, can be framed within a static approach based on the lower bound theorem of limit analysis. As regards the mechanical behaviour of stone, Heyman's hypotheses are adopted (Heyman, 1966), i.e., the blocks of stone composing the structure have infinite compressive strength, and zero tensile strength at the interfaces; moreover, sliding between the blocks cannot occur. Heyman formulates such assumptions by re-evaluating pre-elastic theories (Coulomb, 1776), and exploiting the methodology proposed by Kooharian (1952) for the limit analysis of masonry structures. The graphical method here adopted, called also the 'stability area method', was originally conceived by the French scholar Durand-Clayé (1867). The procedure allows for determining the set of lines of thrust that verify both equilibrium conditions and strength requirements, by

drawing a region in the thrust-eccentricity plane, called the area of stability, representing the domain of statically admissible solutions. This method, originally applied to the assessment of symmetric masonry arches subjected to symmetric load conditions (Durand-Clayé, 1867), was extended also to the analysis of masonry domes of revolution (Durand-Clayé, 1880). In recent years, Aita, Barsotti, and Bennati (2019a) have revisited and re-formulated Durand-Clayé's approach in terms of internal forces, by rigorously framing it within the theoretical background of limit analysis. In (Aita, Barsotti, and Bennati, 2017; 2019b), this approach is further re-elaborated to assess the equilibrium of domes of revolution subjected to their self-weight, by highlighting some inconsistencies of Durand-Clayé's treatment as regards masonry domes (Durand-Clayé, 1880).

In this section, a computerized re-visitation of the *stability area* method is formulated, using an appositely developed algorithm implemented in "Mathematica". The method allows examining the equilibrium of domes subjected to their self-weight, assuming Heyman's hypotheses, according to which Durand-Clayé's method corresponds to a graphical representation of Coulomb's approach (Coulomb, 1776). Without pretending to be exhaustive, the procedure is briefly outlined. As regards the analysis of masonry arches, the stability area (Figure 13a) is a region of the (P, ξ) plane, where P is the horizontal thrust acting at the ideal vertical crown section, while ξ defines the vertical distance of its line of action with respect to a selected reference point (for example, the centre of gravity of the vertical crown section; in this case, ξ coincides with the eccentricity of P). The red/blue curves in the (P, ξ) plane correspond to the attainment of the positive/negative limit bending moment at a given joint. The stability area is obtained by intersecting all the rotational domains thus obtained for each joint. The shape of this area provides useful information on the safety degree of an arch. Under Heyman's hypotheses, when the *stability area* is an extended region of the (P, ξ) plane, see the green region in Figure 13a, infinite admissible solutions are found, corresponding to the points (P, ξ) of this area which in turn identify a set of infinite thrust lines; when the *stability area* vanishes, i.e., shrinks to a single point, a collapse condition identifying the rotational collapse mode 1 (Figure 13b) or 2 (Figure 13c) occurs. According to collapse mode 1 (Figure 13b), starting from the crown section, an extrados hinge (red dot), an intrados hinge (blue dot), and an extrados hinge (red dot) are formed. According to collapse mode 2 (Figure 13c), an intrados hinge (blue dot), an extrados hinge (red dot), and an intrados hinge (blue dot) are formed. Any extrados/intrados hinge corresponds to the attainment of the positive/negative limit bending moment.

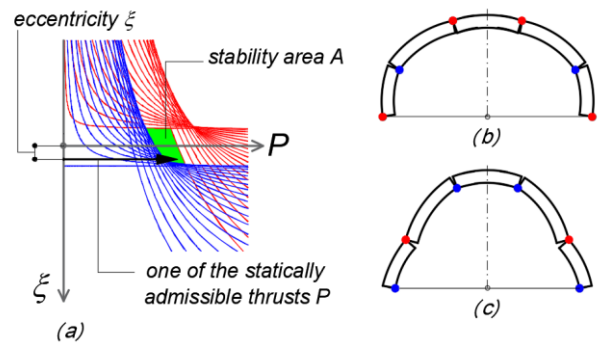


Figure 13. The stability area related to a stable case (a). Collapse modes 1 (b). Collapse mode 2 (c).

As regards domes, the procedure is more complex. Theoretically, domes can have enhanced stability compared to arches, thanks to the formation of hoop stresses along the parallels. However, the weak tensile strength of the material causes meridional cracking, the lower portion of the dome divides into lune, and the hooping action along the parallels is lost. Each resulting lune behaves like one-half of a symmetric arch of variable width (Heyman, 1977; Oppenheim, 1989; Como, 2016). Consequently, a horizontal thrust at the base of the dome arises. To assess whether the dome maintains equilibrium despite the cracking, two analyses need to be performed. Firstly, Durand-Claye's method can be applied initially to each of the lunes composing the dome, studied as independent arches. Then, the method needs to be modified to take into account the action of hoop forces and to correctly assess the collapse condition. This is performed by evaluating if the collapse mechanism identified for the single lune, corresponding to the vanishing of the stability area, is kinematically admissible also for the entire dome (for further details, see Aita, Barsotti, and Bennati, 2017; 2019b; Aita, 2022).

4.2. Equilibrium analysis of conical domes

A first analysis is conducted on the *tholos* roof by assuming that the dome has a conical shape, according to the geometry described in (Hoepfner, 2000). The specific weight assumed for stone/marble is 26 kN/m^3 .

Three hypotheses are examined (Figure 14): (a) the roofing dome covers the surface of the *tholos* entirely and is supported by the external colonnade; (b) the dome has a central *oculus* with a radius corresponding to that of the internal wall, and is supported by the external colonnade; (c) the dome covers only the internal portion of the *tholos*, and is supported by the circular wall.

As regards the geometrical parameters, the arrangement of the stone elements is not known, but two hypotheses are made on the thickness in the vertical direction, $h = 0.14 \text{ m}$ and $h = 0.21 \text{ m}$, obtained from the geometry of the tiles shown in Figure 2. The aperture of the cone is defined by angle 2β , with $\beta = 76.19^\circ$ (Figure 15). The joints separating the stone blocks are assumed for simplicity to be orthogonal to the generatrix line of the cone. The base and cap radii defining the conical dome are read from the geometry of the peristyle and of the cell (Figure 3), and set respectively equal to $R_b = 5.85 \text{ m}$, $R_c = 0$ for case (a); $R_b = 5.85 \text{ m}$, $R_c = 3.53 \text{ m}$ for case (b); $R_b = 3.53 \text{ m}$, $R_c = 0 \text{ m}$ for case (c), see Figure 14.

As regards the collapse conditions, the mechanical behaviour of stone conical domes is similar to that of domes of revolution with a curved profile. Thus, the procedure outlined in Section 4.1 is applied and described more in detail with reference both to the conical dome and to the system composed of the conical dome and the vertical supports.

The starting point consists in considering the dome as the assemblage of lunes of amplitude ζ (Figure 14), according to the 'slicing technique' approach (Heyman, 1977), so that any single lune can be modelled as one-half of an independent arch and its equilibrium assessed. As regards the conical domes under examination, the position of the columns has been considered; thus, $\zeta = 18^\circ$ for cases (a) and (b); $\zeta = 36^\circ$ for case (c) are assumed. In order to identify a limit condition, a meaningful parameter is chosen, for example, the vertical thickness of the stone roof, h (Figure 15). By progressively decreasing the value of the thickness, a limit condition corresponding to the vanishing of the stability area is attained. If the vanishing of the stability area related to the single lune (or to the lune-column system) corresponds to the collapse mode 1 (Figure 16a,b), the entire dome (or the dome-colonnade system) is in a condition of incipient collapse, since collapse mode 1 is kinematically admissible both for the single lune and for the dome as a whole.

On the contrary, if the vanishing of the stability area related to the independent lune identifies the collapse mode 2 (Figure 16c), this collapse mode is not kinematically admissible for the entire dome, since it would require interpenetration of material between adjacent lunes prevented by the action of compressive hoop forces. The collapse of the dome is then searched by further decreasing the thickness until the stability area identifies a mechanism corresponding to collapse mode 1.

The analysis conducted on the conical domes studied separately from the colonnade (or from the vertical supporting structure), allows for concluding that this kind of structure is stable, provided the thrust is balanced by the horizontal reaction exerted by an appropriate constraint (or hoop reinforcement). For all the three cases represented in Figure 14, both values hypothesized for the thickness, $h = 0.14 \text{ m}$ and $h = 0.21 \text{ m}$, are less than the value corresponding to the occurrence of the collapse mode 2, kinematically admissible only for the single lune, not for the entire dome (Figure 16c). By progressively decreasing the thickness, the examination of the stability area shows that the activation of a collapse mechanism according to mode 1 is not possible for conical domes.

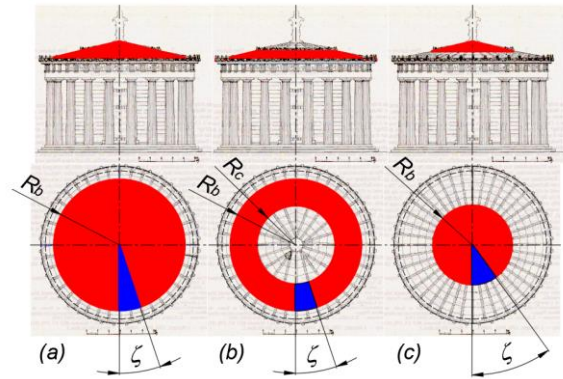


Figure 14. Three hypotheses of conical dome: (a) the dome covers the surface of the *tholos*; (b) the dome has a central *oculus*; (c) the dome covers the internal portion of the *tholos*.

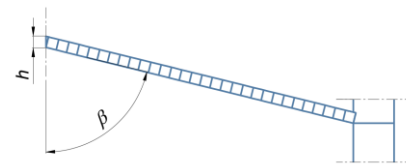


Figure 15. Geometrical parameters: vertical thickness, h , and aperture of the cone, defined by angle 2β .

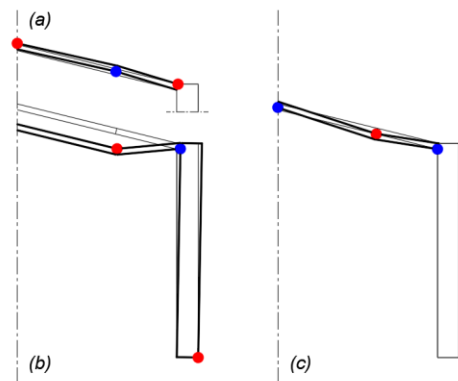


Figure 16. Collapse mode 1 for the conical dome (a); collapse mode 1 for the dome-colonnade system (b); collapse mode 2 (c), kinematically admissible only for an independent lune.

In Figure 17a, the area of stability related to the conical dome of Figure 14a is plotted, by assuming $h = 0.21$ m. In the analysis, the conical dome is divided into 30 elements of equal length (with reference to the generatrix line of the intrados conical surface). For the assumed value of h , the area of stability does not identify statically admissible solutions for the independent lune. However, the conical dome - examined separately from the colonnade - has not reached a collapse condition, since the solution corresponding to the highest extrados hinge (see the green point in Figure 17a) does not match the occurrence of the collapse mode 1. By considering the corresponding thrust line, plotted in Figure 18a, this solution identifies an extrados hinge (the red dot), and an intrados hinge at the conical dome's springing (the blue dot). As regards the upper portion of the dome, it should be observed that the thrust line related to the independent lune would exit at some joints. Considering the action of hoop forces, for example, according to the procedure described in (Aita, Barsotti, and Bennati, 2019b) or in (Paris, Ruscica, and Mirabella Roberti, 2021), allows for finding fully statically admissible solutions for the conical dome.

On the contrary, the results related to the systems formed by the conical dome and the external colonnade (or the vertical load-bearing structure), show that these structures would collapse according to the collapse mode 1, since the horizontal thrust deriving from the meridian cracking of the dome is not compatible with the rotational equilibrium. As an example, the stability area (Figure 17b) related to the case of Figure 14a, with $h = 0.21$ m, shows that statically admissible solutions are not found for the dome-colonnade system. In the analysis, the column has been divided into 5 blocks of the same height. The thrust line corresponding to the highest extrados hinge of the conical dome exits from the profile of the column, by identifying critical horizontal joints (see the pressure centres represented by the red dots in Figure 18b). This condition matches the collapse of the structure according to mode 1 (Figure 16b).

Similar results are obtained for the dome-columns systems related to the cases plotted in Figures 14b and 14c, with $h = 0.14$ m and $h = 0.21$ m, omitted here for the sake of brevity. Increasing the slope of the generatrix lines of the cone or the weight of the vertical elements (for example the *acroteria*) improves the stability of the structure. In any case, the corrective actions indicated above do not seem compatible with plausible architectural solutions.

5. CONCLUDING REMARKS

Starting from the hypothesis of reconstruction of a double roof suggested by archaeologists for the *tholos* of Athena Pronaia in Delphi, this paper examines the structural plausibility of a wooden structure where its stone tiles do not have any structural role and that of a stone structure where the tiles are structural elements that work in compression. The research demonstrates that the hypothesis of a wooden structure is reasonable, although it could present some critical issues from a structural point of view, of which a detailed examination is provided. As far as the stone structure hypothesis is concerned, the conical shape of the roof is not compatible with the equilibrium of the dome-colonnade system, by assuming that the dome is unreinforced. As demonstrated elsewhere with reference to the geometry of the *tholos* (Pizzigoni, Paris and Beatini, 2022), a spherical dome with *oculus* would allow for better structural behaviour, and value the structural role of possible *acroteria*. This may be further studied, above all for the possibility of the tiles functioning as interlocking elements, which could reduce the horizontal thrust and allow the equilibrium of the dome-colonnade system.

Other interesting hypotheses have been developed by archaeologists, that could not have been discussed in the limits of

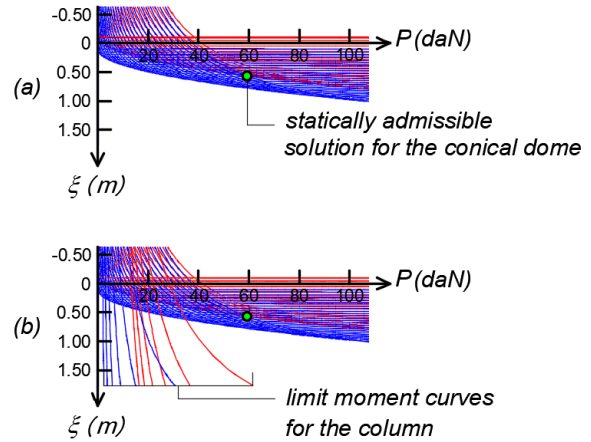


Figure 17. Statically admissible solutions in the (P, ξ) plane according to the stability area method: (a) for the conical dome, (b) for the dome-colonnade system (no solutions are found).

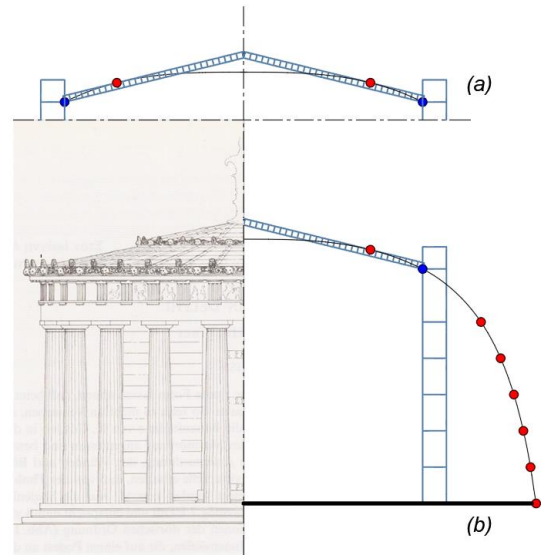


Figure 18. The thrust line corresponding to the green point of the (P, ξ) plane of Figure 17: (a) for the conical dome, (b) for the dome-colonnade system.

this paper. The diversity of the hypotheses shall come with no surprise. Many construction techniques, originated or developed in the Mediterranean area in ancient times, went dismissed for diverse reasons, not necessarily due to poor structural behaviour or architectural quality (Beatini and Tasora, 2021). The paper does not intend to provide a definitive answer to this issue, but in exploring some possible solutions under a structural viewpoint, it illustrates how an integrated approach may help in the hypothesis's formulation and validation. Meanwhile, today, the archaeological site of Delphi is object of the Delphi4Delphi project, an ambitious reconstruction campaign (Liritzis, et al. 2016) aimed at documenting and educational purposes. Technological and structural studies may help identifying which elements a detailed survey may focus on, contributing to an effective usage of resources. The results of this research, therefore, while not being conclusive, act as a stimulus for interdisciplinary collaboration between archaeological, survey, architectural, and structural studies.

REFERENCES

- Aita, D., 2022. Revisiting Classic Methods for the Equilibrium Analysis of Masonry Arches and Domes. In: Milani, G., Sarhosis, V. (eds) *From Corbel Arches to Double Curvature Vaults*. Research for Development. Springer, Cham.
- Aita, D., Barsotti, R., Bennati, S., 2017. A modern reinterpretation of Durand-Claye's method for the study of equilibrium conditions of masonry domes. *AIMETA 2017 - Proceedings of the XXIII Conference of the Italian Association of Theoretical and Applied Mechanics*, Gechi Edizioni, Milano, 1459–1471.
- Aita, D., Barsotti, R., Bennati, S., 2019a. Looking at the collapse modes of circular and pointed masonry arches through the lens of Durand-Claye's stability area method. *Archive of Applied Mechanics*, 89, 1537–1554.
- Aita, D., Barsotti, R., Bennati, S., 2019b. Studying the dome of Pisa cathedral via a modern reinterpretation of Durand-Claye's method. *Journal of Mechanics of Materials and Structures*, 14(5), 603–619, DOI: 10.2140/jomms.2019.14-5.
- Beatini, V., Tasora, A., 2020. Early experimentations within the masonry barrel vault. In Proceedings of IASS Annual Symposia (Vol. 2020, No. 24, pp. 1-11). International Association for Shell and Spatial Structures (IASS).
- Bommelaer, J.-F. 2008. Recherches récentes à Delphes. *Bulletin de la Société Française d'Archéologie Classique* (XXXVIII, 2006-2007), *Revue archéologique*, 2008/1 (n° 45), 161-217.
- Bousquet, J., 1993. La tholos de Delphes et les mathématiques préeuclidiennes. *Bulletin de correspondance hellénique*. Volume 117, livraison 1, 1993, 285-313.
- Charbonneaux, J., and Gottlob, K., 1925. *Le sanctuaire d'Athéna Pronaia (Marmaria)*. Fouilles De Delphes. Tome II, Topographie et Architecture / École Française D'Athènes.
- Como, M., 2016. *Statics of Historic Masonry Constructions*. Springer Series in Solid and Structural Mechanics, vol 5. Springer, Cham.
- Coulomb, C.A., 1776. Essai sur une application des règles de maximis et minimis à quelques problèmes de statique, relatifs à l'architecture. *Mémoires de Mathématique et de Physique, Présentés à l'Académie Royale des Sciences par Divers Savans (année 1773)*, 343–382.
- Durand-Claye, A. 1867. Note sur la vérification de la stabilité des voûtes en maçonnerie et sur l'emploi des courbes de pression. *Annales des Ponts et Chaussées*, 13, 63–93.
- Durand-Claye A., 1880. Vérification de la stabilité des voûtes et des arcs. Applications aux voûtes sphériques, *Annales des Ponts et Chaussées*, 19(1), 416-440.
École Française d' Athènes, 2015. *Guide de Delphes, Le site*, Paris.
- Garavaglia, E., Pizzigoni, A., Sgambi, L., and Basso, N., 2013. Collapse behaviour in reciprocal frame structures. *Structural Engineering and Mechanics*, 46, 533-547.
- Heyman, J., 1977. *Equilibrium of shells structures*, Oxford University Press, Oxford.
- Hoepfner, W., 2000. Zur Tholos in Delphi, *Archäologischer Anzeiger*, 99-107.
- Ito, J. et al., 2004. *New Measurements and Observations of the Treasury of Massalioetes, the Doric Treasury and the Tholos in the Sanctuary of Athena Pronaia at Delphi*, Architectural Mission to Greece Kumamoto University, 2 Vol., Tokyo, Kyushu Univ. Press, 2004. ISBN 4-87378-815-3
- Kooharian, A., 1952. Limit analysis of voussoir (segmental) and concrete arches. *J. Am. Concr. Inst.* 24(4), 317–328.
- Kristensen, C., and Kirkegaard, P. H. 2013. Towards an improved architectural quality in contemporary architecture. In *Structures and Architecture*, 2148-2155. CRC Press.
- Heyman, J., 1966. The stone skeleton. *Int. J. Solids Struct.*, 2(2): 249–279.
- Liritzis, I., Pavlidis, G., Vosynakis, S., Koutsoudis, A., Volonakis, P., Petrochilos, N., Levy, T., 2016. Delphi4Delphi: First results of the digital archaeology initiative for ancient Delphi, Greece. *Antiquity*, 90(354).
- Oppenheim, I.J., Gunaratnam, D.J., Allen, R.H, 1989. Limit state analysis of masonry domes. *Journal of Structural Engineering, ASCE*, 1989; 115(4): 868–882.
- Orlandos, A.K., 1949. Notes on the Roof Tiles of the Parthenon, *Hesperia Supplements*, 1949, Vol. 8, Commemorative Studies in Honor of Theodore Leslie Shear (1949), 259-267+462
- Paris, V., Ruscica, G., Mirabella Roberti, G., 2021. Graphical Modelling of Hoop Force Distribution for Equilibrium Analysis of Masonry Domes. *Nexus Netw J* 23, 855–878.
- Pizzigoni, A., 2023. *Osservando i marmi bianchi della Tholos di Delphi. Perché sono crollati i templi greci?*. Christian Marinotti Edizioni.
- Pizzigoni, A., Beatini, V., and Paris, V., 2022. The Stone Roof. Marble Tholos Tiles in the Sanctuary of Athena Pronaia at Delphi. Stereotomy and Compression Resistant Forms [...], *Structural*, 240, Paper 08, March - April.
- Pizzigoni, A., Paris, V., and Beatini, V., 2022. Why Did Ancient Hellenic Temples Collapse? The Case Study: Athena Pronaia Tholos at Delphi. In Proceedings of the IASS 2022 Symposium affiliated with APCS 2022 conference.
- Roux, G. 1952. Le toit de la Tholos de Marmaria et la couverture des monuments circulaires grecs. *Bulletin de correspondance hellénique*. Volume 76, 1952. 442-483; doi : <https://doi.org/10.3406/bch.1952.2461>
- Tarryn, A. 2018. *Greek Tholoi of the Classical and Hellenistic Periods: An Examination*, Major Paper Essay submitted to the Graduate Program in Classics in conformity with the requirements for the Degree of Master of Arts, Queen's University, Kingston, Ontario, Canada.
- Tokmakidis, K., Ito, J., Mamoto, E., Mori, F., 1998. Detail Surveys with Close-Range Photogrammetry in Archaeological Sites. *International Archives of Photogrammetry and Remote Sensing*, Vol. XXXII, Part 5. Hakodate, 648-651.